Rotational Analysis of Some CO_2 Emission Bands. Part I

By R. F. SCHMID
Ryerson Physical Laboratory, University of Chicago

By using the light of a hollow cathode discharge and that of a Back box with direct current, the red degraded CO_2 bands at λλ3247, 3254, 3370, 3377, 3503, 3511, 3534, 3545, 3674 and 3839A have been photographed in the third order of a 21 foot Rowland grating and analyzed. The bands are composed of *P* and *R* branches and on first inspection they show no alternately missing lines. The lines of the bands at λλ3254, 3377, 3511, 3534, and 3839A show staggering, while the lines of the other bands do not (in the limit of observational accuracy). The single structure of the bands indicates that the molecule is linear in both initial and final states. The distance between the carbon and an oxygen atom computed from the rotational constants is almost the same as computed from the CO and CO^+ bands. The above enumerated bands show no Zeeman effect of the observable lines. Other bands which are found to show more complicated structure and Zeeman effect will be the subject of further investigations.

EXPERIMENTAL

AS ALREADY reported,[1] the emission spectrum of CO_2 can be obtained in suitable intensity by pumping tank CO_2 quickly through a Back box, using a direct current discharge, the magnet pole-pieces serving as cathodes and a piece of tungsten between them as the anode. Besides the strong CO_2 bands, the plates show the entire, but weaker CO^+ spectrum, the third positive CO bands and rather strong angstrom bands. To suppress the CO and CO^+ bands the CO_2 pressure was kept about 4–6 cm Hg and the gas-streaming was made as fast as possible (the use of a *Hypervac* pump brought some success in that direction). The CO_2 consumption was about 5–6 kg per day exposure. In starting with low gas pressure and low current and gradually increasing both and by using magnetic field strengths over 12,000 gauss, the discharge could be kept on one of the magnet pole-pieces with a maximal current of 700–800 milliamperes. In this way the luminosity was enough to give strong third order pictures with the 21 foot grating in 50 hours exposure-time.

As already mentioned[1] some of the CO_2 bands show magnetic effects, and because the discharge in the Back box could not be concentrated on the one pole-piece front in suitable intensity without magnetic fields, it seemed necessary to find another source, which would give a strong CO_2 spectrum without any magnetic field. The steel hollow-cathode in the arrangement sketched in Fig. 1 was fastened in the center of a three liter bulb, the neck of which was cooled. A steel anode was placed 5 cm away from the cathode. This arrangement gave very satisfactory results in respect to CO_2 luminosity and relative weakness of CO and CO^+ bands. Of course, the spectrum contained some iron lines also, but no other metal could be used because of the high CO_2 pressure. Graphite, aluminum, tin, etc., burned away in a short time.

[1] R. F. Schmid, Phys. Rev. **39**, 589 (1932).

Some considerations (see below) showed it desirable to determine the effective emission temperature of the source used, which could be done by studying the rotational intensity distribution of certain well-known bands

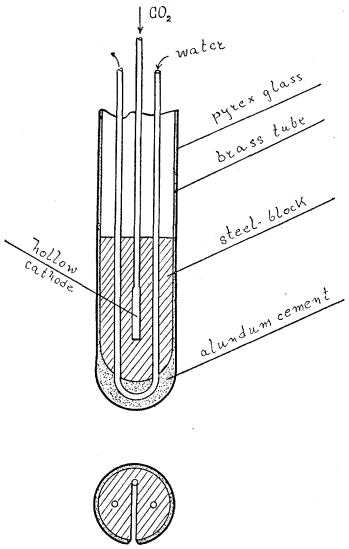

Fig. 1. Steel hollow cathode water-cooled and with direct gas-inlet in the hollow part itself.

present in the spectra. The λ 4835A, 0→1 angstrom band, having clear background and only a few overlappings, was especially suitable for that purpose and showed the maximal intensity in its P branch at $K''_{max}=15$ in the Q branch at $K''_{max}=14$ and in the R branch at $K''_{max}=13$. By using the formulas:[2]

$$P \text{ branch} \qquad kT = B'(K_{max}'' - 1)(2K_{max}'' - 1)$$

$$Q \text{ branch} \qquad kT = B'\tfrac{1}{2}(2K_{max}'' + 1)^2$$

$$R \text{ branch} \qquad kT = B'(K_{max}'' + 2)(2K_{max}'' + 3)$$

(where k is the Boltzmann factor and $B'=1.94$ cm^{-1}), it was found, in very good agreement for all the three branches: $kT=800$ cm^{-1}, that is $T=870$°C.

Besides that, having pictures on which (due to leaks) the λ3914A (0→0) and λ4278 (0→1) N_2^+ bands were also present, in which bands the maximum seemed to be between $K''_{max}=12$ for the stronger half R branch and $K''_{max}=13$ for the weaker odd numbered set, we have, by using the formula[3]

$$kT = B'(K_{max}'' + 1)(2K_{max}'' + 3)$$

with $B'=2.07$ cm^{-1} the value $kT=845$ cm^{-1} slightly higher than the above given one for CO, in agreement with what seems to be usual for ionized molecules.[4]

[2] F. London and H. Hönl, Zeits. f. Physik **33,** 803 (1925).
[3] R. S. Mulliken, Phys. Rev. **30,** 138 and 785 (1927).
[4] L. S. Ornstein, Zeits. f. Physik **49,** 315 (1928).

Results

The most recent report on the CO_2 emission spectrum—on the basis of low-dispersion photographs, however—was given by Smyth.[5] Comparing the pictures given by him in his Fig. 2, parts *a* and *b*, with the present plates, some differences were noticed, which are due probably to differences in methods of excitation.

(1) Smyth's electron beam discharge seems to be cooler than the present one, which gives better developed bands and is more suitable for rotational analysis purposes, while his pictures are more useful for a vibrational analysis.

(2) According to Smyth: . . . "from λ2900 to λ3500 the bands occur in five well-defined groups . . . from 3500 to 4000 is a terrific tangle." In the present pictures however, the bands from λ3500 to λ4000, as well as those from λ2900 to λ3500 fall into well-defined groups, four in number (at λλ3503, 3661, 3839 and 3905) in the former region.

(3) The electron beam method picture shows very strong bands at 3853, 3871 and 3961A. The present pictures show the two first mentioned bands much less intense and in the place of the third (about 3961A) they show practically nothing. Also the groups at 4108A and longer wave-lengths are weaker on the present plates.

Concerning the rotational fine structure, the present high-dispersion plates show that the strongest bands of the part of the spectrum which falls into groups, namely the bands λλ3247, 3254, 3370, 3377, 3503, 3511, 3534, 3545, 3674, and 3839A, all have the same simple structure, except that some show staggering and others do not (see below); they can be analyzed into *P* and *R* branches; *Q* branches could not be detected. The simple band structure indicates that the molecule is linear in both upper and lower energy states. The absence of a *Q* branch may be explained by assuming only such transitions, in which the orbital-angular momentum quantum number (in diatomic molecules Λ) does not change: $\Sigma\rightarrow\Sigma$, $\Pi\rightarrow\Pi$, etc. transitions.

Comparing pictures taken with and without magnetic fields, we find that the lines of the above-enumerated bands show no Zeeman effect. Other bands: λλ2880∼2900A and λ3661A, which differ from the above-mentioned bands in having more complicated structure also without fields, show up to the highest rotational states shiftings, broadenings, and in some places also splittings and polarizations in the magnetic field.

Calculations on the basis of the Zeeman effect energy level formula suitable for a diatomic molecule[6]

$$\Delta\nu = \Delta\nu_{\text{normal}} \cdot [M/K(K+1)]\Lambda^2$$

with $M=-K, -(K-1) \ldots (K-1)\ K$ show that, assuming a $^1\Pi\rightarrow{}^1\Pi$ transition ($\Lambda=1$), we would get for 30,000 gauss field strength for the line $P(5)$ an overall width of the patterns $\Delta\nu=0.16$ cm^{-1}, where, however, the intense components cover a width only of 0.06 cm^{-1}; for $P(9)$ we get an overall width

[5] H. D. Smyth, Phys. Rev. **38**, 2 000 (1931) and **39**, 380 (1932).

[6] J. S. Millis, Phys. Rev. **38**, 1148 (1931).

$\Delta\nu = 0.04$ cm^{-1}. In the case of a $^1\Delta \rightarrow {}^1\Delta$ transition ($\Lambda = 2$), we would get four times larger widths.

Now on the present plates the lines with the lowest rotational quantum number that can be observed are usually P lines from $P(7)$ or $P(9)$ up and R lines from $R(17)$ or $R(19)$ up. Only in two bands, λ3370 and λ3503A, where the overlappings with neighboring strong R lines are fewer, can we observe (without field) P lines from $P(3)$ or $P(4)$ up. The widths of the lines were found to be about 0.04 cm^{-1} and we may suppose that a broadening of the same magnitude in a magnetic field probably would be detected. However, the only observable effect of the magnetic field seems to be to cause a more

TABLE I. λ = *3503A*.

P		*R*		*P*		*R*		*P*	
M	ν(cm^{-1})	*M*	ν(cm^{-1})	*M*	ν(cm^{-1})	*M*	ν(cm^{-1})	*M*	ν(cm^{-1})
2	28,530.47?	18	28,534.92	23	28,498.12	39	28,511.12	44	28,438.77
3	29.58	19	34.37	24	96.02	40	9.24	45	35.30
4	28.54	20	33.84	25	93.78	41	7.56	46	31.71
5	27.55	21	33.00	26	91.50	42	5.44	47	28.11
6	26.39	22	32.49	27	89.10	43	3.54	48	24.37
7	25.22	23	31.78	28	86.65	44	1.53	49	20.51
8	23.99	24	30.94	29	84.10	45	499.37	50	16.82
9	22.72	25	30.05	30	81.50	46	97.14	51	13.05
10	21.40	26	29.09	31	78.83	47	94.85	52	08.78
11	19.96	27	28.07	32	76.12	48	92.57	53	05.06
12	18.52	28	26.96	33	73.31	49	90.18	54	01.27
13	17.03	29	25.87	34	70.56	50	87.88	55	396.88
14	15.43	30	24.67	35	67.59	51	85.35	56	92.73
15	13.77	31	23.43	36	64.65	52	82.69	57	88.39
16	12.01	32	22.09	37	61.66	53	80.18	58	84.15
17	10.28	33	20.73	38	58.72	54	77.47	59	79.79
18	08.42	34	19.32	39	55.43	55	74.80	60	74.86
19	06.47	35	17.81	40	52.14	56	72.03	61	70.80
20	04.71	36	16.24	41	48.90			62	66.29
21	02.49	37	14.64	42	45.64			63	61.65
22	00.41	38	12.87	43	42.29			64	56.87

TABLE II. λ = *3370A*.

P		*R*		*P*		*R*		*P*	
M	ν(cm^{-1})	*M*	ν(cm^{-1})	*M*	ν(cm^{-1})	*M*	ν(cm^{-1})	*M*	ν(cm^{-1})
3	29,656.18?	17	29,661.57	21	29,628.58	35	29,642.77	39	29,580.40
4	55.17	18	61.01	22	26.47	36	41.19	40	77.11
5	54.18	19	60.58	23	24.26	37	39.36	41	73.72
6	52.99	20	59.86	24	22.01	38	37.69	42	70.21
7	51.83	21	59.18	25	19.62	39	35.85	43	66.90
8	50.56	22	58.44	26	17.28	40	33.89	44	63.29
9	49.26	23	57.60	27	14.80	41	31.85	45	59.74
10	47.88	24	56.74	28	12.27	42	29.92	46	55.90
11	46.43	25	55.78	29	09.69	43	27.86		
12	44.95	26	54.80	30	07.08	44	25.61		
13	43.40	27	53.69	31	04.38	45	23.49		
14	41.78	28	52.50	32	01.50	46	21.11		
15	40.21	29	51.33	33	598.79	47	18.85		
16	38.32	30	50.06	34	95.90	48	16.30		
17	36.49	31	48.75	35	92.94	49	13.37		
18	34.61	32	47.34	36	89.82	50	11.34		
19	32.68	33	45.91	37	86.73	51	9.60		
20	30.69	34	44.41	38	83.45	52	7.11		

rapid decrease of intensity in the P branch in the direction of lower rotational quantum numbers. This may probably be attributed to an unresolved Zeeman splitting increasing in that direction. With field (25,400 gauss) the first observable P lines are about $P(8)$ or $P(9)$ in the above two bands. The widths of all the *observable* lines with field is the same (within observational accuracy) as without field.

TABLE III. $\lambda = 3247A$.

P		R	P		R	P	
M	$\nu(\text{cm}^{-1})$	M	M	$\nu(\text{cm}^{-1})$	M	M	$\nu(\text{cm}^{-1})$
	30,781.60	21	20	30,752.93	41	40	30,698.18
	80.59	22	21	50.76	42	41	94.74
	79.79	23	22	48.64	43	42	91.07
	78.83	24	23	46.36	44	43	87.64
	77.80	25	24	44.14	45	44	84.11
	76.67	26	25	41.72	46	45	80.37
	75.58	27	26	39.27	47	46	76.67
	74.39	28	27	36.73	48	47	72.61
	73.17	29	28	34.20	49	48	68.88
9	71.81	30	29	31.58	50	49	65.02
10	70.38	31	30	28.83	51	50	60.91
11	68.95	32	31	26.01	52	51	56.67
12	67.41	33	32	23.19	53	52	52.49
13	65.84	34	33	20.25	54	53	48.81
14	64.24	35	34	17.36	55	54	44.82
15	62.49	36	35	14.19	56	55	40.17
16	60.72	37	36	11.29	57	56	36.29
17	58.91	38	37	07.95	58	57	31.87
18	56.96	39	38	04.78	59	58	27.47
19	54.93	40	39	01.44			

TABLE IV. $\lambda = 3511A$.

	P		R		P		R
M	$\nu(\text{cm}^{-1})$	M	$\nu(\text{cm}^{-1})$	M	$\nu(\text{cm}^{-1})$	M	$\nu(\text{cm}^{-1})$
13	28,453.14	17	28,471.54	28	28,422.85	32	28,458.72
14	51.24	18	71.16	29	20.51	33	57.63
15	49.85	19	70.62	30	17.84	34	56.09
16	47.93	20	69.97	31	15.19	35	54.81
17	46.32	21	69.68	32	12.55	36	53.14
18	44.60	22	68.86.	33	09.95	37	51.72
19	42.60	23	68.23	34	07.08	38	49.85
20	40.55	24	67.36	35	04.35	39	48.30
21	38.71	25	66.46	36	01.27	40	46.32
22	36.51	26	65.58	37	398.55	41	44.60
23	34.45	27	64.65	38	95.09	42	42.60
24	32.17	28	63.44	39	92.27		
25	30.01	29	62.35	40	89.08		
26	27.67	30	61.33	41	85.96		
27	25.62	31	60.12				

Considering these facts, we may conclude, that a $^1\Delta \rightarrow {}^1\Delta$ transition seems to be improbable, while the possibility of a $^1\Pi \rightarrow {}^1\Pi$ transition, and of course of a $^1\Sigma \rightarrow {}^1\Sigma$ transition (which should show no Zeeman effect) remain.

The bands beyond 3845A appear to be not much more complicated than the above-enumerated ten bands and also have no observable Zeeman effect, but there is so much overlapping that a third order picture does not permit their analysis into branches.

The present paper deals with the analysis of the ten bands enumerated above. Tables I to X contain the measurements of the bands. The accuracy

TABLE V. $\lambda = 3377A$.

P		R		P		R	
M	$\nu(cm^{-1})$	M	$\nu(cm^{-1})$	M	$\nu(cm^{-1})$	M	$\nu(cm^{-1})$
8	29,585.78	17	29,596.93	33	29,534.39	42	29,566.26
9	84.51	18	96.37	34	31.35	43	64.41
10	83.27	19	95.90	35	28.52	44	62.11
11	81.91	20	95.22	36	25.44	45	60.10
12	80.40	21	94.75	37	22.50	46	57.61
13	78.67	22	93.86	38	19.32	47	55.62
14	76.71	23	93.03	39	16.16	48	52.89
15	75.24	24	92.26	40	12.82	49	50.90
16	73.47	25	91.33	41	09.72	50	48.43
17	71.70	26	90.33	42	06.14	51	45.83
18	69.77	27	89.43	43	02.89	52	42.87
19	67.89	28	88.10	44	499.25	53	40.46
20	65.87	29	87.01	45	95.69	54	37.22
21	63.95	30	85.78	46	91.99	55	35.04
22	61.64	31	84.70	47	88.50	56	31.87
23	59.74	32	83.45	48	84.52	57	29.01
24	57.09	33	81.91	49	80.90	58	25.87
25	54.98	34	80.40	50	76.92	59	23.06
26	52.89	35	79.06	51	73.12	60	19.62
27	50.31	36	77.11	52	68.96		
28	47.74	37	75.70	53	64.97		
29	45.22	38	73.72	54	60.83		
30	42.43	39	72.09	55	56.78		
31	39.89	40	70.21	56	52.22		
32	37.09	41	68.38	57	48.19		

TABLE VI. $\lambda = 3254A$.

P		R		P		R	
M	$\nu(cm^{-1})$	M	$\nu(cm^{-1})$	M	$\nu(cm^{-1})$	M	$\nu(cm^{-1})$
6	30,708.77	17	30,717.36	29	30,665.02	40	30,689.08
7	07.59	18	16.75	30	62.28	41	87.12
8	06.41	19	16.17	31	59.69	42	84.76
9	04.78	20	15.63	32	56.67	43	82.97
10	03.68	21	14.93	33	53.96	44	80.37
11	02.15	22	14.19	34	50.86	45	78.36
12	00.60	23	13.31	35	48.10	46	75.78
13	699.20	24	12.26	36	44.82	47	73.63
14	97.51	25	11.29	37	41.64	48	70.95
15	95.91	26	10.17	38	38.39	49	68.13
16	93.88	27	09.27	39	35.33	50	65.57
17	92.14	28	07.95	40	31.87	51	63.37
18	90.19	29	06.84	41	28.61	52	60.28
19	88.36	30	05.38	42	24.82	53	57.82
20	86.07	31	04.25	43	21.47	54	54.61
21	84.11	32	02.64	44	18.08	55	51.96
22	82.01	33	01.44	45	14.31	56	48.81
23	79.86	34	699.62	46	10.30	57	45.82
24	77.44	35	98.18	47	06.90	58	42.56
25	75.13	36	96.30	48	02.72	59	39.74
26	72.61	37	94.70	49	598.99	60	36.29
27	70.26	38	92.68	50	94.84	61	33.40
28	67.60	39	91.07				

of the pure measurement is of the same order as that of the iron lines in that region serving as normals, i.e., a few thousandths of an angstrom unit or in

TABLE VII. $\lambda = 3534A$.

P		R		P		R	
M	$\nu(cm^{-1})$	M	$\nu(cm^{-1})$	M	$\nu(cm^{-1})$	M	$\nu(cm^{-1})$
9	28,275.43	17	28,288.23	25	28,247.12	33	28,273.99
10	73.99	18	87.75	26	44.69	34	72.76
11	72.76	19	87.13	27	42.41	35	71.34
12	71.34	20	86.62	28	39.69	36	69.47
13	69.79	21	86.00	29	37.45	37	68.37
14	68.37	22	85.45	30	34.64	38	66.28
15	66.74	23	84.80	31	32.39	39	64.88
16	64.88	24	84.00	32	29.68	40	62.86
17	63.27	25	83.12	33	27.19	41	61.18
18	61.18	26	82.13	34	23.99	42	59.02
19	59.55	27	81.21	35	21.49	43	57.43
20	57.43	28	80.12	36	18.28	44	54.97
21	55.65	29	79.06	37	15.54	45	53.43
22	53.43	30	77.79	38	12.28	46	50.71
23	51.49	31	76.74	39	09.42		
24	49.23	32	75.43	40	06.03		

TABLE VIII. $\lambda = 3545A$.

R		P		R		P	
$\nu(cm^{-1})$	M	M	$\nu(cm^{-1})$	M	M	$\nu(cm^{-1}$	
28,195.81	17	9	28,182.91	32	23	28,158.68	
95.33	18	10	81.67	33	24	56,53	
94.88	19	11	80.19	34	25	54.22	
94.24	20	12	78.69	35	26	51.87	
93.70	21	13	77.23	36	27	49.72	
92.87	22	14	75.67	37	28	47.10	
92.26	23	15	74.04	38	29	44.77	
91.43	24	16	72.28	39	30	42.09	
90.60	25	17	70.45	40	31	39.65	
89.75	26	18	68.83		32	36.84	
88.71	27	19	66.84		33	34.26	
87.65	28	20	64.84		34	31.38	
86.67	29	21	62.88		35	28.58	
85.53	30	22	60.81		36	25.62	
84.24	31						

TABLE IX. $\lambda = 3674A$.

R		P		R		P	
$\nu(cm^{-1})$	M	M	$\nu(cm^{-1})$	M	M	$\nu(cm^{-1})$	
27,205.77	18		27,195.54	31	20	27,175.44	
05.38	19		94.38	32	21	73.53	
04.82	20	9	93.24	33	22	71.57	
04.32	21	10	92.22	34	23	69.46	
03.69	22	11	91.48	35	24	67.36	
03.04	23	12	89.44	36	25	65.20	
02.28	24	13	88.00	37	26	62.76	
01.60	25	14	86.48	38	27	60.56	
00.64	26	15	83.94	39	28	58.16	
199.82	27	16	82.26	40	29	55.94	
98.83	28	17	80.76		30	53.66	
97.74	29	18	79.18		31	50.87	
96.71	30	19	77.17		32	48.15	

TABLE X. $\lambda = 3839A$.

P				*R*			
M	back	Δ	forth	*M*	back	Δ	forth
5			26,030.72	16	26,039.70		
		1.13				0.29	
6	26,029.59			17			26,039.41
		0.89				0.35	
7			028.70	18	039.06		
		1.27				0.46	
8	027.43			19			038.60
		1.22				0.39	
9			026.21	20	038.21		
		1.33				0.53	
10	024.88			21			037.68
		1.30				0.60	
11			023.58	22	037.08		
		1.44				0.57	
12	022.14			23			036.51
		1.46				0.71	
13			020.68	24	035.80		
		1.47				0.69	
14	019.21			25			035.11
		1.56				0.85	
15			017.65	26	034.26		
		1.63				0.77	
16	016.02			27			033.49
		1.66				1.01	
17			014.36	28	032.48		
		1.78				0.93	
18	012.58			29			031.55
		1.77				1.07	
19			010.81	30	030.48		
		1.88				1.02	
20	008.93			31			029.46
		1.88				1.24	
21			007.05	32	028.22		
		2.05				1.01	
22	005.00			33			027.21
		1.92				1.50	
23			003.08	34	025.71		
		2.14				1.09	
24	000.94			35			024.62
		2.07				1.58	
25			25,998.87	36	023.04		
		2.04				1.24	
26	25,996.83			37			021.80
		2.38				1.74	
27			994.45	38	020.06		
		2.36				1.23	
28	992.09			39			018.83
		2.25				1.79	
29			989.84	40	017.04		
		2.60				1.44	
30	987.24			41			015.60
		2.33				1.98	
31			984.91	42	013.62		
		2.75				1.49	
32	982.16			43			012.13
		2.33				2.11	
33			979.83	44	010.02		
		2.83				1.53	
34	977.00			45			008.49
		2.53				2.21	
35			974.47	46	006.18		
		2.97				1.62	

TABLE X. (Continued)
$\lambda = 3839A$

P				R			
M	back	Δ	forth	M	back	Δ	forth
36	25,971.50			47			26,004.56
		2.65				2.47	
37			25,968.85	48	26,002.09		
		3.15				1.72	
38	965.70			49			000.37
		2.67				2.54	
39			963.03	50	25,997.83		
		3.09				1.82	
40	959.94			51			25,996.01
		2.87				2.72	
41			957.07	52	993.29		
		3.22				1.85	
42	953.85			53			991.44
						2.90	
				54	988.54		
						1.97	
				55			986.57
						3.02	
				56	983.55		

wave numbers $\pm 0.03 \sim 0.04$ cm^{-1}. Unfortunately, however, the overlappings are very frequent in these bands and this—together with the extraordinary closeness of the lines—causes some errors which, especially in the combination differences, in the worst cases give deviations up to ± 0.5 cm^{-1} which, however, are not systematic.

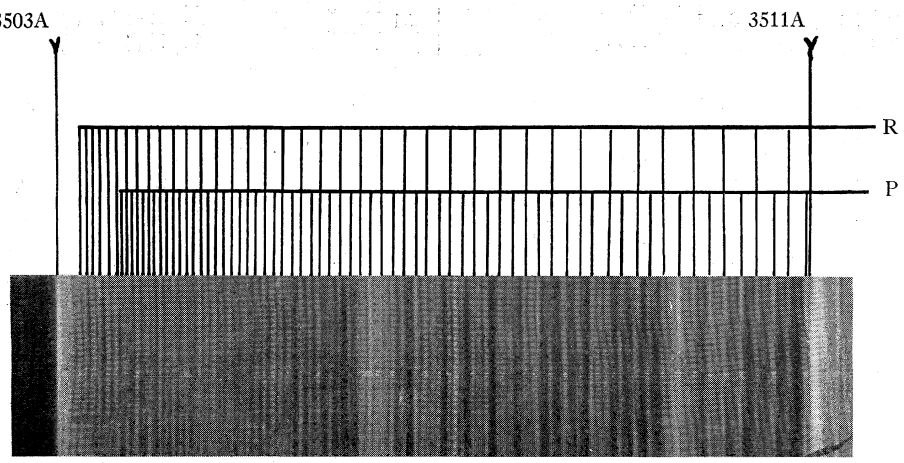

Fig. 2. Non-staggering CO_2 band at λ3503A.

Five of the measured bands, those at λλ3254, 3377, 3511, 3534 and 3839A show staggering, i.e., the lines of the branches are slightly displaced alternately toward lower and toward higher frequencies; the five others, in the limit of the observational accuracy do not. The staggering increases with the rotational quantum number. This phenomenon, together with the fact that

in the same or nearly the same place on the plates we have always P and R lines differing in rotational quantum number by 22–25 units, gives the impression that the P lines form a smooth series, while the R lines stagger back and forth between them. The measurements show, however, that the successive differences between adjacent P lines also alternate. To illustrate this fact, in Table X, for the band at λ3839A—which shows the staggering most prominently—these successive differences are listed in addition to the wave numbers. The rotational numbering of the lines listed in Table I–X should be taken as arbitrary. Some considerations (see below) show, however, that the true rotational numbering probably does not differ from that here given by more than a few units at most.

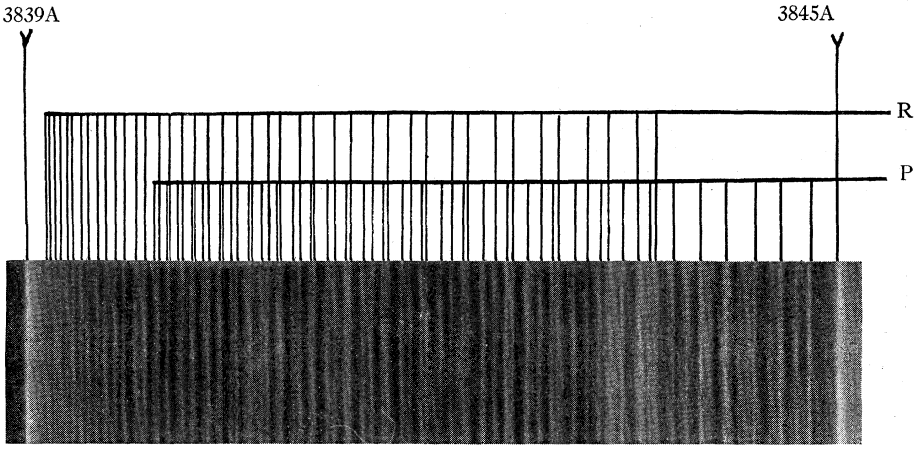

Fig. 3. Staggering CO_2 band at λ3839A.

A striking feature of the investigated bands may be mentioned now. This is: if we calculate differences between P and R lines, such as $R(M-2)-P(M)$ $R(M-1)-P(M)$, and so forth, we find that all the ten bands give almost the same sets of numbers. To illustrate this fact, in Table XI are listed the differences called $R(M)-P(M)$ for all bands. These differences are linear functions of M. At the bottom we find the values B, the constant coefficient (divided by four) of the in M linear sets. These, and B values calculated in other similar tables for several other difference sets, agree for all the ten bands within 0.004 cm^{-1}. This fact formed the common basis for the M numbering in all ten bands.

Since the time of their discovery, most of the CO_2 bands in the region here investigated have been believed to be members of v' progressions. The evidence for this opinion is that the wave numbers of the heads of most bands can be interpreted by the formula

$$\nu_{\text{head}} = \nu_a + 1136.85v' - 1.85v'^2 \qquad (1)$$

where v' is a vibrational quantum number. The different progressions have for ν_a different values (see Smyth[5] especially). The fact that the red degraded,

TABLE XI.

	Supposed $R(M)$–$P(M)$ combinations for all bands									
λ	3247	3254	3370	3377	3503	3511	3534	3545	3674	3839
		stagg.		stagg.		stagg.	stagg.			stagg.
M										
15										
16										23.68
17		25.22	25.08	25.23		25.22	25.17	25.36		25.05
18		26.56	26.40	26.60	26.50	26.56	26.57	26.50	26.59	26.48
19		27.81	27.90	28.01	27.90	28.02	27.58	23.04	28.21	27.79
20		29.56	29.17	29.35	29.13	29.42	29.19	29.40	29.38	29.28
21	30.84	30.82	30.60	30.80	30.51	30.97	30.25	30.82	30.79	30.63
22	31.95	32.18	31.97	32.22	32.08	32.35	31.82	32.06	32.12	32.08
23	33.43	33.45	33.34	33.29	33.66	33.78	33.31	33.58	33.58	33.43
24	34.69	34.82	34.73	35.17	34.92	35.19	34.77	34.90	34.92	34.86
25	36.08	36.16	36.16	36.35	36.27	36.45	36.00	36.38	36.40	36.24
26	37.40	37.56	37.52	37.44	37.59	37.91	37.44	37.88	37.88	37.43
27	38.85	39.01	38.89	39.12	38.97	39.02	38.80	38.99	39.26	39.04
28	40.19	40.35	40.23	40.44	40.31	40.59	40.43	40.55	40.67	40.39
29	41.59	41.82	41.64	41.79	41.77	41.84	41.61	41.90	41.80	41.71
30	42.98	43.10	42.98	43.35	43.17	43.49	43.15	43.44	43.05	43.24
31	44.37	44.56	44.37	44.81	44.60	44.93	44.35	44.59	44.67	44.55
32	45.76	45.97	45.84	46.36	45.97	46.17	45.75	46.07	46.23	46.06
33	47.16	47.48	47.12	47.52	47.42	47.68	46.80	47.41		47.38
34	48.48	48.76	48.51	49.05	48.76	49.01	48.77	48.81		48.71
35	50.05	50.08	49.83	50.54	50.22	50.46	49.85	50.11		50.15
36	51.20	51.48	51.37	51.67	51.59	51.87	51.19	51.61		51.54
37	52.77	53.10	52.63	53.20	52.98	53.17	52.83			52.95
38	54.13	54.29	54.24	54.40	54.15	54.76	54.00			54.36
39	55.52	55.74	55.45	55.93	55.69	56.03	55.46			55.80
40	56.75	57.21	56.78	57.39	57.10	57.24	56.83			57.10
41	58.19	58.51	58.13	58.66	58.66	58.64				58.53
42	59.69	59.94	59.71	60.12	59.80					59.77
43	61.00	61.50	60.96	61.52	61.25					
44	62.25	62.59	62.32	62.86	62.76					
45	63.77	64.05	63.75	64.41	64.07					
46	65.05	65.48	65.21	65.62	65.43					
47	66.66	66.73		67.12	66.74					
48	67.85	68.23		68.37	68.20					
49	69.18	69.14		70.00	69.67					
50	70.67	70.73		71.51	71.06					
51		72.54		72.71						
52		73.65		73.91						
53		75.02		75.49						
54		76.43		76.39						
55		77.94		78.26						
56		79.53		79.65						
B	0.3467	0.3473	0.3464	0.3485	0.3482	0.3495	0.3468	0.3493	0.3497	0.3484

simple-structured CO_2 bands, and their lines themselves also, can be fitted in sets with almost the same constants, from the vibrational as well as from the rotational viewpoint, is one of the most prominent features of these bands, especially considering that a completely rigorous analysis has not yet been possible.

Among the ten bands here investigated there are three staggering and three non-staggering bands which form successive members of two v'progressions:

λλ3503, 3370, 3247A . . . non-staggering

λλ3511, 3377, 3254A . . . staggering.

To get the rotational numbering it therefore seemed suitable to look for identical sets of final state combination differences. The results of computations of this kind are given in Tables XII and XIII for the staggering and non-staggering sets, respectively.

In Table XII, best agreement is found in the set marked $R(M-2)-P(M)$. If we call this set $R(J-1)-P(J+1)$ and calculate the rotational constants as usual with the formula:

$$\Delta_2 T''(J) = R(J-1) - P(J+1) = 4B''(J+\tfrac{1}{2}) \qquad (2)$$

we get the surprising result, that the J values are (within limits of a few hundredths, which may be attributed to experimental error) half integers. The two neighboring sets $R(M-1)-P(M)$ and $R(M-3)-P(M)$, however, give whole numbers for J. It will be seen that the sets $R(M-1)-R(M+1)$ give almost as good agreements as $R(M-2)-R(M)$, while other sets give gradually increasing deviations which soon pass outside the range of possible experimental errors. Hence the correct combination set is probably not far different from $R(M-2)-P(M)$. If integral J values are assumed to be necessary, it is probably $R(M-1)-P(M)$. In any case, however, since the the calculated B'' values do not vary much from one set to another, the B'' value obtained from, say, $R(M-1)-P(M)$ is probably not far from correct. It also follows that the B' values are not very different from (slightly less than) the B'' values. For instance if $R(M-1)-P(M)$ gives $4B''(J\mp 1/2)$, then $R(M+1)-P(M)=4B'(J+1/2)$. If we assume this we find that the B' values occur in succession as

$$B'_{3511} > B'_{3377} > B'_{3254}$$

in harmony with the vibrational numbering[5]

$$v'_{3511} < v'_{3377} < v'_{3254},$$

if we assume the formula well known for diatomic molecules:

$$B_v = B_0 - \alpha(v+\tfrac{1}{2})$$

with positive α, as is plausible for v' progressions with formula (1). The values for α seem to be very small, of the order of magnitude of 0.001 cm^{-1}. To this may be attributed the difficulty in deciding which combination sets are the correct ones. The alternate occurrence of whole and half J numbers for various possible combinations is marked in the right-hand corner of each combination in Tables XII and XIII.

Concerning Table XIII it should be mentioned that the data in the λ3247A band are in all probability not so accurate as those for the two others, because this band is composed of coincident P and R branches (at least for the eye), which among other things, results in a lower accuracy. Namely, the coinciding P and R lines have rotational quantum numbers differing by about 22 units, so that the coinciding components have not at all the same intensity and they contribute to the resulting line in unequal proportion and so a systematic shifting of the measured resulting line, i.e., of its center

TABLE XII. *Possible combinations in the staggering progressions.*

	$R(M-3)-P(M)$: *whole*			$R(M-2)-P(M)$: *half*			$R(M-1)-P(M)$: *whole*			$R(M)-P(M)$: *half*			$R(M+1)-P(M)$: *whole*		
M	3511	3377	3254	3511	3377	3254	3511	3377	3754	3511	3377	3254	3511	3377	3254
16													23.61	23.46	23.48
17										25.22	25.23	25.22	24.84	24.67	24.61
18							26.94	27.16	27.17	26.56	26.60	26.56	26.02	26.13	25.98
19				28.94	29.04	29.00	28.56	28.48	28.39	28.02	28.01	27.81	27.37	27.33	27.27
20	30.99	31.06	31.29	30.61	30.50	30.68	30.07	30.03	30.10	29.42	29.35	29.56	29.13	28.88	28.86
21	32.45	32.42	32.64	31.91	31.95	32.06	31.26	31.27	31.52	30.97	30.80	30.82	30.15	29.91	30.08
22	34.11	34.26	34.16	33.46	33.58	33.62	33.17	33.11	32.92	32.35	32.22	32.18	31.72	31.39	31.30
23	35.52	35.48	35.77	35.23	35.01	35.07	34.41	34.12	34.33	33.78	33.29	33.45	32.91	32.42	32.40
24	37.51	37.66	37.49	36.69	36.77	36.75	36.06	35.94	35.87	35.19	35.17	34.82	34.29	34.24	33.85
25	38.85	38.88	39.06	38.22	38.05	38.18	37.35	37.28	37.13	36.45	36.35	36.16	35.57	35.35	35.04
26	40.56	40.14	40.70	39.69	39.37	39.65	38.79	38.44	38.68	37.91	37.44	37.56	36.98	36.54	36.66
27	41.74	41.95	42.00	40.84	41.02	41.03	39.96	40.02	39.89	39.02	39.12	39.01	37.82	37.79	37.69
28	43.61	43.59	43.69	42.73	42.59	42.57	41.80	41.69	41.67	40.59	40.44	40.35	39.50	39.27	39.24
29	45.07	45.11	45.15	44.14	44.21	44.75	42.93	42.88	42.93	41.84	41.79	41.82	40.82	40.56	40.36
30	46.81	47.00	46.99	45.60	45.67	45.67	44.51	44.58	44.56	43.49	43.35	43.10	42.28	42.27	41.97
31	48.25	48.21	48.26	47.16	47.12	47.15	46.14	45.89	45.69	44.93	44.81	44.56	43.53	43.56	42.95
32	49.80	49.92	50.17	48.78	48.69	48.71	47.57	47.61	47.58	46.17	46.36	45.97	45.08	44.82	44.77
33	51.38	51.39	51.42	50.17	50.31	50.29	48.77	49.06	48.68	47.68	47.52	47.48	46.14	46.01	45.66
34	53.04	53.35	53.39	51.64	52.10	51.78	50.55	50.56	50.58	49.01	49.05	48.76	47.73	47.71	47.32
35	54.37	54.93	54.54	53.28	53.39	53.34	51.74	51.88	51.52	50.46	50.54	50.08	48.79	48.59	48.20
36	56.36	56.47	56.62	54.82	54.96	54.80	53.54	53.62	53.36	51.87	51.67	51.48	50.45	50.26	49.88
37	57.54	57.90	57.98	56.26	56.56	56.54	54.59	54.61	54.66	53.17	53.20	53.10	51.30	51.22	51.04
38	59.72	59.74	59.79	58.05	57.79	57.91	56.63	56.38	56.31	54.76	54.40	54.29	53.21	52.77	52.68
39	60.87	60.95	60.97	59.45	59.54	59.41	57.58	57.56	57.35	56.03	55.93	55.74	54.05	54.05	53.75
40	62.64	62.88	62.83	60.77	60.90	60.81	59.22	59.27	59.20	57.24	57.39	57.21	55.52	55.56	55.25
41	63.89	64.00	64.07	62.44	62.37	62.46	60.36	60.49	60.47	58.64	58.66	58.51	56.64	56.54	56.15
42		65.95	66.25		64.07	64.26		62.24	62.30		60.12	59.94		58.27	58.15
43		67.32	67.61		65.49	65.65		63.37	63.29		61.52	61.50		59.22	58.90
44		69.13	69.04		67.01	66.68		65.16	64.89		62.86	62.29		60.85	60.28
45		70.57	70.45		68.72	68.66		66.42	66.06		64.41	64.05		61.92	61.47
46		72.42	72.67		70.12	70.07		68.11	68.06		65.62	65.48		63.63	63.33
47		73.61	73.47		71.60	71.46		69.11	68.88		67.12	66.73		64.39	64.05
48		75.58	75.64		73.09	73.06		71.10	70.91		68.37	68.23		66.38	65.41
49		76.71	76.79		74.72	74.64		71.99	71.96		70.00	69.14		67.53	66.58
50		78.70	78.79		75.97	76.11		73.98	73.29		71.51	70.73		68.91	68.53
51		79.77	80.12		77.78	77.30		74.31	74.74		72.71	72.54		69.75	69.45
52		81.94	81.50		79.47	78.94		76.87	76.74		73.91	73.65		71.50	71.19
53		83.46	82.77		80.86	80.57		77.90	77.48		75.49	75.02		72.25	71.81
54		85.00	85.19		82.04	82.10		79.63	79.64		76.39	76.43		74.21	73.78
55		86.09	86.26		83.68	83.80		80.44	80.59		78.26	77.94		75.09	74.79
56		88.24	88.54		85.00	85.33		82.82	82.68		79.65	79.53		76.79	76.54
57		89.03			86.85			83.68			80.82			77.68	
	average difference -0.11		average difference -0.06	average difference -0.02		average difference -0.01	average difference $+0.02$		average difference $+0.08$	average difference $+0.08$		average difference $+0.19$	average difference $+0.16$		average difference $+0.22$
B even	0.3942	0.3974	0.3986	0.3801	0.3800	0.3799	0.3768	0.3764	0.3758	0.3498	0.3485	0.3472	0.3464	0.3449	0.3431
B odd	0.3927	0.3960	0.3958	0.3798	0.3802	0.3800	0.3749	0.3742	0.3733	0.3493	0.3486	0.3474	0.3443	0.3430	0.3410
possible combinations		Δ_2T''			Δ_2T''			Δ_2T'			Δ_2T'			Δ_2T'	

Note to this table. The explanation of B_{even} and B_{odd} is given in the text together with the explanation of the same signs in Table XIV.

TABLE VIII. *Possible combinations in the non-staggering progression.*

M	$R(M-3)-P(M)$: *whole* 3503	3370	3247	$R(M-2)-P(M)$: *half* 3503	3370	3247	$R(M-1)-P(M)$: *whole* 3503	3370	3247	$R(M)-P(M)$: *half* 3503	3370	3247	$R(M+1)-P(M)$: *whole* 3503	3370	3247
16														23.25	
17											25.08		24.64	24.52	
18								26.96		26.50	26.40		25.95	25.97	
19					28.89		28.45	28.33		27.90	27.90		27.37	27.18	
20		30.88		30.21	30.32		29.66	29.89		29.13	29.17		28.29	28.49	28.67
21	32.43	32.43		31.88	32.00		31.35	31.28		30.51	30.60	30.84	30.00	29.86	29.83
22	33.96	34.11		33.43	33.39		32.59	32.71	32.96	32.08	31.97	31.95	31.37	31.13	31.15
23	35.72	35.60		34.88	34.92	35.24	34.37	34.18	34.23	33.66	33.34	33.43	32.82	32.48	32.47
24	36.98	37.17	37.46	36.47	36.43	36.45	35.76	35.59	35.65	34.92	34.73	34.69	34.03	33.77	33.66
25	38.71	38.82	38.87	38.00	37.98	38.07	37.16	37.12	37.11	36.27	36.16	36.08	35.31	35.18	34.95
26	40.28	40.32	40.52	39.44	39.46	39.56	38.55	38.50	38.53	37.59	37.52	37.40	36.57	36.41	36.31
27	41.84	41.94	42.10	40.95	40.98	41.07	39.99	40.00	39.94	38.97	38.89	38.85	37.86	37.70	37.66
28	43.40	43.51	43.60	42.44	42.53	42.47	41.42	41.42	41.38	40.31	40.23	40.19	39.22	39.06	38.97
29	44.99	45.11	45.09	43.97	44.00	44.00	42.86	42.81	42.81	41.77	41.64	41.59	40.57	40.37	40.23
30	46.57	46.61	46.75	45.46	45.42	45.56	44.37	44.25	44.34	43.17	42.98	42.98	41.93	41.67	41.55
31	48.13	48.12	48.38	47.04	46.95	47.16	45.84	45.68	45.80	44.60	44.37	44.37	43.26	42.96	42.94
32	49.75	49.83	49.98	48.55	48.56	48.62	47.31	47.25	47.19	45.97	45.84	45.76	44.61	44.41	44.22
33	51.36	51.27	51.56	50.12	49.96	50.13	48.78	48.55	48.70	47.42	47.12	47.16	46.01	45.62	45.59
34	52.87	52.85	53.02	51.53	51.44	51.59	50.17	50.01	50.05	48.76	48.51	48.48	47.25	46.87	46.88
35	54.50	54.40	54.76	53.14	52.97	53.22	51.73	51.47	51.65	50.22	49.83	50.05	48.65	48.25	48.30
36	56.08	56.09	56.12	54.67	54.59	54.55	53.16	52.95	52.95	51.59	51.37	51.20	49.99	49.54	49.43
37	57.66	57.68	57.89	56.15	56.04	56.29	54.58	54.46	54.54	52.98	52.63	52.77	51.21	50.96	50.96
38	59.09	59.32	59.46	57.52	57.74	57.71	55.92	55.91	55.94	54.15	54.24	54.13	52.40	52.40	52.18
39	60.81	60.79	61.05	59.21	58.96	59.28	57.44	57.29	57.47	55.69	55.45	55.52	53.81	53.49	53.49
40	62.50	62.25	62.54	60.73	60.58	60.73	58.98	58.74	58.78	57.10	56.78	56.75	55.42	54.74	54.75
41	63.97	63.97	64.17	62.22	62.13	62.22	60.34	60.17	60.19	58.66	58.13	58.19	56.54	56.20	56.02
42	65.48	65.64	65.89	63.60	63.68	63.86	61.92	61.64	61.86	59.80	59.71	59.69	57.90	57.65	57.57
43	66.95	66.99	67.29	65.27	64.95	65.29	63.15	63.02	63.12	61.25	60.96	61.00	59.24	58.71	58.72
44	68.79	68.56	68.82	66.67	66.63	66.65	64.77	64.57	64.53	62.76	62.32	62.25	60.60	60.20	60.03
45	70.14	70.18	70.39	68.24	68.12	68.27	66.23	65.87	66.99	64.07	63.75	63.77	61.84	61.37	61.35
46	71.83	71.96	71.97	69.82	69.71	69.69	67.66	67.59	67.47	65.43	65.21	65.05	63.14	62.95	62.60
47	73.42		73.75	71.26		71.53	69.03		69.11	66.74		66.66	64.46		64.12
48	75.00		75.26	72.77		72.84	70.48		70.39	68.20		67.85	65.81		65.32
49	76.63		76.70	74.34		74.25	72.06		71.71	69.67		69.18	67.37		66.56
50	78.03		78.36	75.75		7 .82	73.36		73.29	71.06		70.67	68.53		67.92
B	0.391	0.391	0.393	0.379	0.379	0.380	0.362	0.360	0.362	0.348	0.346	0.346	0.332	0.328	0.328

average difference −0.03 (3503 → 3370) · average difference −0.19 (3370 → 3247)
average difference +0.04 (3503 → 3370) · average difference −0.12 (3370 → 3247)
average difference +0.12 (3503 → 3370) · average difference −0.07 (3370 → 3247)
average difference +0.19 (3503 → 3370) · average difference −0.003 (3370 → 3247)
average difference +0.26 (3503 → 3370) · average difference +0.06 (3370 → 3247)

possible combinations

- Δ_2T'' (3503 → 3247)
- Δ_2T'' (3370 → 3503)
- Δ_2T' (3503 → 3247)
- Δ_2T' (3503 → 3370)
- Δ_2T'' (3370 → 3247)
- Δ_2T' (3370 → 3247)

of gravity, may occur. Hence, less weight should be given to agreements involving the combination sets of this band.

In this table we may say that the supposed common final state may be interpreted by one of the left-hand columns. Anyway, we find that the numbering calculated on the basis of formula (2) does not differ from our arbitrary numbering by more than one or two (or by a half or one and a half) units .This is true for both progressions, and in view of Table XI, probably for all the bands. The B values for both initial and final states then probably lie within the interval of: $0.395 \sim 0.345$ cm^{-1}.

On the basis of these values, assuming the rotational axis perpendicular to the line through the three atoms of CO_2 and going through the carbon atom and assuming the effective mass for that axis:

$$\mu = 2M_{\text{oxygen}} = 53.12 \cdot 10^{-24}\text{g},$$

we can roughly calculate the distance between the carbon and one of oxygen atoms. We get in this way: r equal to about $1.25 \sim 1.15 \cdot 10^{-8}$ cm, that is, almost the same as, or slightly larger than, in the CO and CO^+ molecules.

In making the above computations concerning the numbering and rotational constants we have not mentioned the theoretical requirement that, because of the symmetry of the CO_2 molecule and the zero nuclear spin of the oxygen atoms, alternate rotational levels and band lines should be missing. As for the staggering bands, a very simple assumption (see below) may explain both staggering and missing lines. But considering only the non-staggering bands, the question might arise whether these bands could not be explained by supposing that they have alternately missing lines, so that the rotational constants would really have values roughly half as large and the rotational quantum numbers of the lines, values roughly twice as large as stated above. In making this assumption, we would encounter difficulties not only in the fact that in this case the nuclear separations would become improbably large, but also in interpreting the rotational intensity distribution of the bands. It was shown before that the intensity distribution of the angstrom bands present in the spectrum gives a value for $kT = 800$ cm^{-1} and assuming the formula

$$kT = B'(K_{\max}'' + 1)(2K_{\max}'' + 3)$$

for the R branches of the CO_2 bands, we would get with supposed B' values about $0.360 \sim 0.350$ (middle and left-hand columns in Table XIII) a value for $K''_{\max}$ about $31 \sim 32$; with B values half as large we get $K''_{\max}$ about $43 \sim 45$. The $R(43)$ or $R(45)$ line would of course be identical with our former lines $R(21) \sim R(23)$. Now the intensity distribution of the bands at λ3503A and λ3370A on several plates was registered with a Moll microphotometer and the curves show, although distorted by the close lying lines and some overlappings also, their maxima undoubtedly within the interval of $M = 30$ to 33. This confirms the assumption that alternate lines are not missing in the bands without staggering.

In surveying all the combinations given in Tables XII and XIII it seemed

of interest to determine whether the two progressions have or have not an exactly common level. Every conceivable kind of combination between the lines of the different bands in the different progressions was tried, but every set obtained showed—to be sure small but systematic deviations from the others.

A simple explanation of the staggering together with the theoretical requirement of missing levels can be given as follows: In analogy to diatomic molecules, we assume that the rotational levels of CO_2 form a set (in the first approximation) with the well-known formula

$$T(J) = BJ(J+1) \text{ or } T(K) = BK(K+1)$$

and in further analogy with diatomic molecules, we assume a splitting of the levels, something like the Λ-type doubling. Now, due to the zero nuclear spins

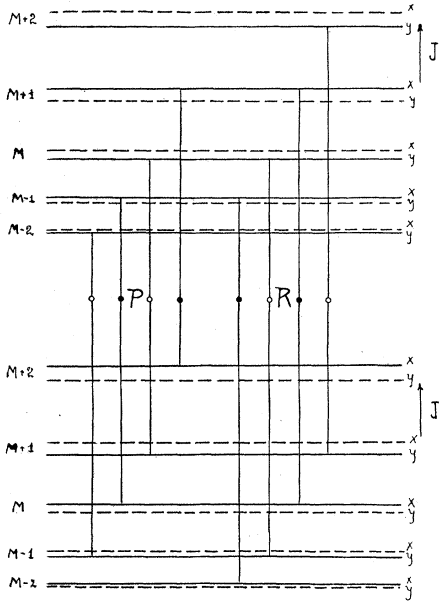

Fig. 4. Possible energy diagram and explanation of the staggering in some CO_2 bands. The rotational levels have doublings in analogy to the Λ-type doublings of a diatomic molecule. Because of the zero nuclear spin of the oxygen atoms, every second level is missing (broken lines). *P* and *R* branches appear to be divided into two alternating sets marked with full and empty circles. To get term-differences, we have to combine full circle *R* lines with full circle *P* lines and empty circle *R* lines with empty circle *P* lines.

of the oxygen atoms, every other level, alternately the upper and lower one of the sublevels of a Λ-like doublet, as in He_2, should be missing. The energy-level diagram could be drawn then somewhat as in Fig. 4 (where the Λ-like doublings are greatly exaggerated).[7] The *P* and *R* lines would then appear to be divided into the two sets, marked with full and empty circles (transitions

[7] See Figs. 17 and 32 for structure of bands like this given by R. S. Mulliken, Rev. Mod. Phys. **3**, 89 (1931).

only between x sublevels and transitions only between y sublevels). To get the x level combinations, we have to combine full circle P and R lines, to get y level combinations, we have to combine empty circle lines. But the question which half of the P and of the R branches represent the empty and which the full circle lines, and therefore which set of P lines should be combined with which set of R lines, remains at first unanswered.

The magnitude of the staggering is different in the different bands. In the band at λ3839A it is the largest, in the progresssion λλ3511, 3377 and 3254A it is less and in the band λ3534 it is only just observable. This suggests that perhaps the non-staggering bands have staggering also, only its magnitude is less than enough to become observable.

The λ3839A band shows the most striking staggering, so it may serve as an example for the following considerations. In Table X the lines of the bands are fitted in two columns, marked "forth" and "back," where the "forth" means a deviation in the direction of higher frequencies, that is, since the band is red-degraded, toward the head, and "back" in the opposite direction. The arbitrary numbering was chosen in such a way that even numbers belong to "back" staggered, odd numbers to "forth" staggered lines in both branches. (This was done also in the other staggering bands, and this served as a second basis, besides that explained by discussing Table XI (see above), for the common M numbering in the different bands.)

Table XIV contains a number of possible combinations in the λ3839 band; combinations in which the M value of the P line is even or odd are listed respectively in the left and right subcolumns of each combination set. Before each combination value is given the value J which is calculated, assuming the formula

$$\textit{combination}\ (R - P) = 4B(J + \tfrac{1}{2})$$

and the average constant differences in each column of two adjacent combination values are listed as "$8B$" at the bottom of the table. The approximate nature of the J values obtained is given at the top of each column under "whole" or "half." (In the bands without staggering, similar tables give almost exactly integers and half integers: cf., data in Tables XII, XIII.) Below these their deviations from the nearest whole and half numbers are also listed. The sum of the deviations for the two halves of each combination set seems to be zero in the "whole" sets. The deviations themselves seem to be two or three times as large in the "whole" combinations as in the "half" ones. The difference $8B_{\text{even}} - 8B_{\text{odd}}$ seems to be about four times as large in the "whole" sets as in the "half" sets, and also differs in sign.

The quantity $8B_{\text{even}} - 8B_{\text{odd}}$ in the other staggering bands also was found to be positive in the "whole" sets in all cases and negative in the "half" sets in most cases. Its magnitude (an approximate measure of the staggering) seems to be about $+0.016$ cm^{-1} in the "whole" sets. The calculated J values are equal to whole and half numbers within the lower observational accuracy—due to frequent overlappings in these bands, and do not permit a real calculation of their deviations from the next whole or half number.

TABLE XIV. *Possible combinations in λ3839A, strongly staggering band.*

	$R(M-2)-P(M)$: half				$R(M-1)-P(M)$: whole				$R(M)-P(M)$: half				$R(M+1)-P(M)$: whole				$R(M+2)-P(M)$: half				
	J	$R-P$	J	$R-P$	J	$R-P$	J	$R-P$	J	$R-P$	J	$R-P$	J	$R-P$	J	$R-P$	J	$R-P$	J	$R-P$	
	0.53		0.43		0.84		0.16		0.54		0.43		0.82		0.17		0.55		0.43		Average of the decimal part of apparent J.
	−0.03		+0.07		+0.16		−0.16		−0.04		+0.07		+0.18		−0.17		−0.05		+0.07		Deviation of apparent J from integers on half integers.
M																					
14																	15.54	20.49			
15															16.14	22.05			16.46	21.76	
16									16.53	23.68			16.85	23.39			17.54	23.04			
17							17.10	25.34			17.44	25.05			18.14	24.70			18.39	24.24	
18	17.52	27.12			17.87	26.83			18.54	26.48			18.80	26.02			19.57	25.63			
19			18.45	28.60			19.12	28.25			19.41	27.79			20.18	27.40			20.44	26.87	
20	19.52	30.13			19.81	29.67			20.55	29.28			20.83	28.75			21.54	28.15			
21			20.40	31.55			21.14	31.16			21.44	30.63			22.16	30.03			22.46	29.46	
22	21.57	33.21			21.87	32.68			22.57	32.08			22.88	31.51			23.61	30.80			
23			22.42	34.60			23.11	34.00			23.45	33.43			24.19	32.72			24.46	32.03	
24	23.52	36.14			23.85	35.57			24.57	34.86			24.85	34.17			25.59	33.32			
25			24.44	37.64			25.14	36.93			25.46	36.24			26.21	35.39			26.48	34.62	
26	25.40	38.97			25.71	38.28			26.41	37.43			26.70	36.66			27.41	35.65			
27			26.44	40.66			27.14	39.81			27.46	39.04			28.20	38.03			28.41	37.10	
28	27.53	42.17			27.84	41.40			28.54	40.39			28.78	39.46			29.56	38.39			
29			28.42	43.65			29.61	42.64			29.38	41.71			30.17	40.64			30.38	39.62	
30	29.57	45.24			29.83	44.31			30.59	43.24			30.82	42.22			31.58	40.98			
31			30.40	46.64			31.14	45.57			31.41	44.55			32.18	43.31			32.46	42.30	
32	31.61	48.32			31.88	47.30			32.62	46.06			32.92	45.05			33.60	43.55			
33			32.38	49.63			33.10	48.39			33.44	47.38			34.12	45.88			34.40	44.79	
34	33.54	51.22			33.87	50.21			34.52	48.71			34.83	47.62			35.54	46.04			
35			34.44	52.74			35.08	51.24			35.42	50.15			36.15	48.57			36.38	47.33	
36	35.53	54.21			35.86	53.12			36.56	51.54			36.82	50.30			37.52	48.56			
37			36.45	55.77			37.13	54.19			37.43	52.95			38.14	51.21			38.45	49.98	
38	37.61	57.34			37.90	56.10			38.59	54.36			38.92	53.13			39.69	51.34			
39			38.44	58.77			39.10	57.03			39.47	55.80			40.26	54.01			40.47	52.57	
40	39.45	60.12			39.81	58.89			40.56	57.10			40.79	55.66			41.53	53.68			
41			40.42	61.76			41.14	59.97			41.43	58.53			42.17	56.55			42.41	55.06	
42	41.49	63.19			41.77	61.75			42.48	59.77			42.74	58.28			43.48	56.17			
$8B$	3.0094		3.0186		2.9215		2.8802		2.7815		2.7921		2.6958		2.6504		2.5546		2.5665		
$8B_{\text{even}}-8B_{\text{odd}}$	−0.0092				+0.0413				−0.0106				+0.0454				−0.0119				

The levels of Λ-type doubling in a diatomic molecule can be interpreted by the formula[8]

$$\phi_i(J) = \kappa_i + \epsilon_i J + \delta_i J(J+1) + \cdots$$

where i refers to either x or y sublevels. We may try to use this formula for the present case.

Combining two sublevels differing by two units in J, but of the same kind (that is, two x, or two y levels) we get

$$\phi_i(J+1) + \phi_i(J-1) = 2\epsilon_i + 4\delta_i(J + \tfrac{1}{2}).$$

The difference between B_{even} and B_{odd} should then represent the difference between δ_x and δ_y, while the deviations of the apparent J's from whole numbers correspond to ϵ_x and ϵ_y, of which according to the observational data one is positive, the other negative. Both the "whole" and the "half" combinations in the band at λ3839A show effective B and J values which are consistent with this scheme, and there seems to be no way of deciding between them on this basis, nor of deciding which of the "whole" or of the "half" combinations is most likely to be correct, except roughly by assuming the intensity distribution to be analogous to that in the bands which belong to progressions.

In a separate paper Professor R. S. Mulliken expects to discuss some further points in connections with the theoretical interpretation of the CO_2 bands.

The writer wishes to express his thankfulness to Professor Robert S. Mulliken for his unceasing advice in analyzing the bands and to Professor George S. Monk for his kind assistance in experimental troubles, especially for the excellent temperature control of the grating-room.

[8] R. S. Mulliken, Rev. Mod. Phys. **3**, 89 (1931).

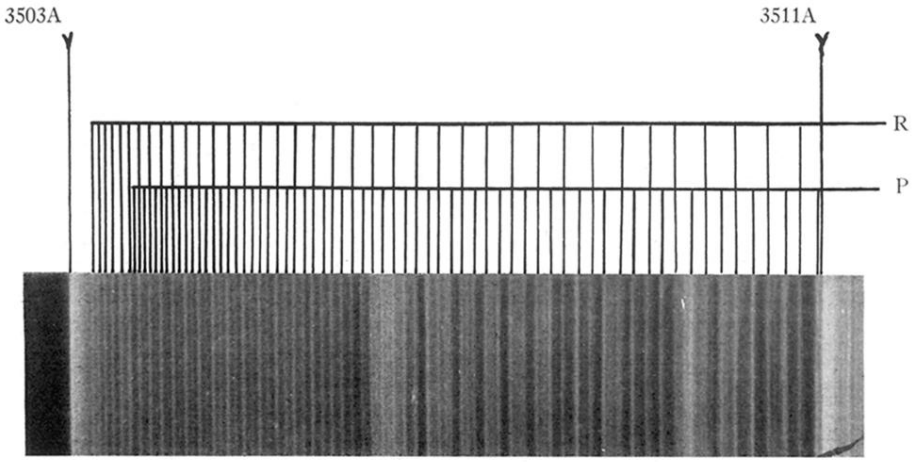

Fig. 2. Non-staggering CO_2 band at λ3503A.

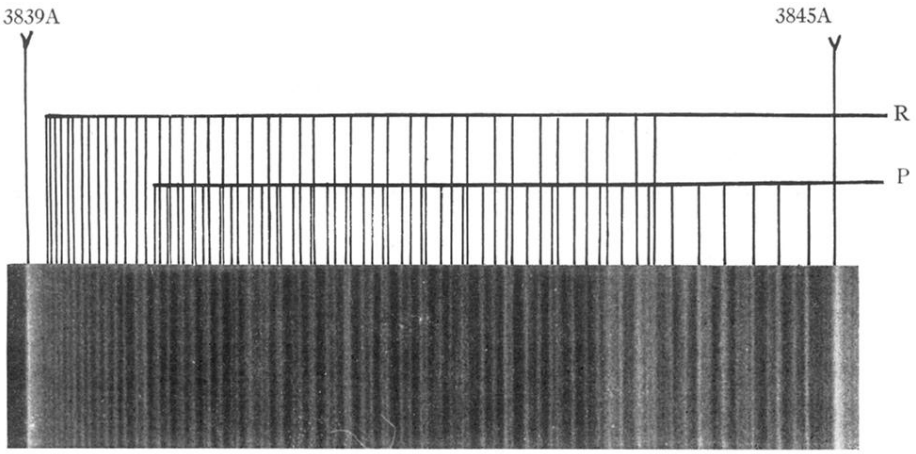

Fig. 3. Staggering CO_2 band at λ3839A.